



## Photocatalytic Activity of Fe and TiO<sub>2</sub> Embedded in a Carbon Matrix

KAN ZHANG<sup>1</sup>, JONG GEUN CHOI<sup>1</sup> and WON CHUN OH<sup>1,\*</sup>

<sup>1</sup>Department of Advanced Materials & Science Engineering, Hanseo University, Chungnam 356-706, South Korea

\*Corresponding author: Fax: (82)(41)6883352; Tel: (82)(41)6601337; E-mail: wc\_oh@hanseo.ac.kr

(Received: 22 March 2010;

Accepted: 28 August 2010)

AJC-9055

Fe and TiO<sub>2</sub> embedded in a carbon matrix composites have been successfully obtained by introduction of a residue or external carbon precursor. Fe and TiO<sub>2</sub> embedded in a carbon cluster as a residue carbon precursor was prepared by heat treatment of C<sub>10</sub>H<sub>10</sub>Fe and C<sub>16</sub>H<sub>36</sub>O<sub>4</sub>Ti mixed at 873 K under oxygen atmosphere. Fe and TiO<sub>2</sub> embedded in multiwalled carbon nanotube (MWCNT) composites were prepared using Fe(NO<sub>3</sub>)<sub>3</sub>, C<sub>16</sub>H<sub>36</sub>O<sub>4</sub>Ti and MWCNT as an external carbon precursor and finally heating at 873 K. The Fe/TiO<sub>2</sub>/carbon composites obtained were characterized from BET, SEM, TEM, XRD and EDX analysis. The methylene blue (MB) solution was used to examine the photocatalytic activity of Fe/TiO<sub>2</sub>/C and Fe/TiO<sub>2</sub>/MWCNT composites. The photocatalytic activity of Fe/TiO<sub>2</sub>/C and Fe/TiO<sub>2</sub>/MWCNT composites was found to be higher than that of the pure TiO<sub>2</sub> and Fe/TiO<sub>2</sub> under UV and visible light irradiation. In comparison of photocatalytic activity of Fe/TiO<sub>2</sub>/C and Fe/TiO<sub>2</sub>/MWCNT composites, the photocatalytic activity of Fe/TiO<sub>2</sub>/MWCNT composites was slightly higher than that of Fe/TiO<sub>2</sub>/C due to strong electronic properties of MWCNT. The photocatalytic activity of Fe/TiO<sub>2</sub>/C and Fe/TiO<sub>2</sub>/MWCNT composites was more progressed fast by powerful H<sub>2</sub>O<sub>2</sub> assisting photo-Fenton reaction due to oxidation of Fe<sup>2+</sup>-Fe<sup>3+</sup> under UV irradiation.

**Key Words:** Fe/TiO<sub>2</sub>/C composites, Fe/TiO<sub>2</sub>/MWCNT composites, Photocatalytic activity, Photo-Fenton.

### INTRODUCTION

Industrial dyestuffs including textile dyes are recognized as being an important environmental threat. Physical, chemical and biological methods are available for treatment of such waste. However, they are not sufficient and advantageous. Therefore, advanced oxidation processes (AOPs), including peroxone, non-thermal plasma, photo-Fenton, UV/O<sub>3</sub>, UV/H<sub>2</sub>O<sub>2</sub> and semiconductor photocatalysis process, have been developed by many researchers to degrade organic compounds, which are suitable for achieving the complete elimination and mineralization of various pollutants<sup>1-4</sup>.

It was reported that combination of photocatalysis and photo-assisted Fenton reaction can give more photocatalytic performance<sup>5,6</sup>. Iron is the most commonly used metal as a Fenton reagent and can be used in the form of iron salt as a homogeneous catalyst or as a heterogeneous catalyst in the form of a supported metal. Therefore, doping of iron to TiO<sub>2</sub> has been widely described by the others, because iron doping can give another some benefits such as retarding the inconvenient recombination reaction, which proceeds after photocatalyst excitation and also can extend the photocatalytic ability of the photocatalyst to the visible region<sup>7,8</sup>. However, it was proved that the Fe/TiO<sub>2</sub> photocatalysts revealed the lower surface area and a lower anatase-to-rutile<sup>9,10</sup>. Recently, Fe/TiO<sub>2</sub> deposited

with carbon was widely developed<sup>11,12</sup>. It was reported that introduction of carbon could improve surface area and suppress the phase transformation from anatase to rutile during heat-treatment at high temperatures, with improving crystallinity of anatase phase, which was responsible for the high photoactivity for the degradation of pollutants in water. It was also reported that Fe/TiO<sub>2</sub> deposited with carbon composites could work in photo-Fenton process under UV irradiation and hydrogen peroxide addition.

Additionally, Kisch *et al.*<sup>13</sup>, synthesized TiO<sub>2</sub>/carbon by a modified sol-gel method exhibited high photocatalytic activity under visible light irradiation. Wang and co-workers reported that MWCNT/TiO<sub>2</sub> prepared from a sol-gel method using titanium alkoxide precursor was able to photodegraded phenol under visible light illumination<sup>14</sup>. Matsui *et al.*<sup>15,16</sup> synthesized TiO<sub>2</sub>/metal oxide/carbon cluster *via* a calcination method and they claimed that carbon doping led to lower band gap and high photocurrent under visible light irradiation. In our previous studies<sup>17,18</sup>, Y or Pt/CNT/TiO<sub>2</sub> composites prepared showed more beneficial effect for improving adsorption ability and photocatalytic activity under the visible light irradiation. Therefore, the higher photocatalytic activity supposed for Fe/TiO<sub>2</sub>/carbon composites can be expected under UV and visible light irradiation.

In this paper, Fe/TiO<sub>2</sub>/carbon photocatalysts with the residue carbon and external carbon were prepared, respectively. The influence of carbon precursor and iron in the photocatalyst on its photocatalytic activity in degradation of methylene blue under UV with and without addition of H<sub>2</sub>O<sub>2</sub> was discussed. In addition, photo-catalytic activity of Fe/TiO<sub>2</sub>/carbon composites with the residue carbon and external carbon was compared under UV and visible light system.

## EXPERIMENTAL

Ferrocene (C<sub>10</sub>H<sub>10</sub>Fe) and phenolic resin (PR) as iron and carbon source for preparation of Fe/TiO<sub>2</sub>/C composite was purchased from Strem Chemicals, New Buryport, USA and KangNam Chemical Co., Ltd. Korean, respectively. Multi-wall carbon nanotube (MWCNT) as the support material for preparation of Fe/TiO<sub>2</sub>/MWCNT composite was purchased from carbon nano-material technology Co., Korea (diameter: *ca.* 20 nm, length: *ca.* 5 μm). *m*-Chloroperbenzoic acid (MCPBA) was used as an oxidized reagent which was purchased from Acros Organics, New Jersey, USA. Benzene (99.5 %) was used as an organic solvent which was purchased from Samchun Pure Chemical Co., Ltd., Korea. The TNB [Ti(OC<sub>4</sub>H<sub>9</sub>)<sub>4</sub>] as a titanium source for the preparation of composites was purchased from Acros Organics, New Jersey, USA. And Fe(NO<sub>3</sub>)<sub>3</sub>·9H<sub>2</sub>O as the ferric source for preparation of Fe/TiO<sub>2</sub>/MWCNT composite was purchased from Duksan Pure Chemical Co., Ltd., (Korea). The methylene blue (99.99+ %) was used as analytical grade which was purchased from Duksan Pure Chemical Co., Ltd., (Korea). Hydrogen peroxide (H<sub>2</sub>O<sub>2</sub>) (35 %) was purchased from Daejung Chemicals & Metals Co., Ltd. (Korea).

**Preparation of samples:** The 3 mL [Ti(OC<sub>4</sub>H<sub>9</sub>)<sub>4</sub>] was dissolved in 20 mL of benzene to prepare the [Ti(OC<sub>4</sub>H<sub>9</sub>)<sub>4</sub>] solution. The 0.1g PR added into the [Ti(OC<sub>4</sub>H<sub>9</sub>)<sub>4</sub>] solution and vigorously stirred for 0.5 h. The 5 mL 0.1 M C<sub>10</sub>H<sub>10</sub>Fe solutions were slowly dropped into the mixed solution prepared and vigorously stirred for 5 h, then the remaining residue was dried at 363 K. Finally, the mixture was heat treated at 873 K. Then the Fe/TiO<sub>2</sub>/C composites were obtained. For preparation of Fe/TiO<sub>2</sub>/MWCNT composites, first, 2 g MCPBA was dissolved in 80 mL benzene. Then, 10 mg MWCNT powder was put into the oxidizing agent solution, refluxed at 353 K for 6 h then the solid precipitates were formed and dried at 363 K. The oxidized MWCNT was added into to 5 mL 0.1 M Fe(NO<sub>3</sub>)<sub>3</sub> solutions and the mixtures were stirred for 24 h using a non-magnetic stirrer at room temperature. After the heat treatment at 773 K, we obtained the Fe-MWCNT. The Fe-MWCNT was put into the [Ti(OC<sub>4</sub>H<sub>9</sub>)<sub>4</sub>] solution prepared as above and then the mixed solution was stirred for 5 h in an air atmosphere. After stirring the solution transformed to gel state and these gels were reacted at 873 K for 1 h. And then the Fe/TiO<sub>2</sub>/MWCNT composites were obtained. The procedure of prepared samples is showed in Fig. 1.

**Characteristics and investigations of the samples:** The BET surface area by N<sub>2</sub> adsorption method was measured at 77 K using a BET analyzer (Monosorb, USA). XRD (Shimadzu XD-D1, Japan) result was used to identify the crystallinity with CuK<sub>α</sub> radiation. SEM was used to observe the surface

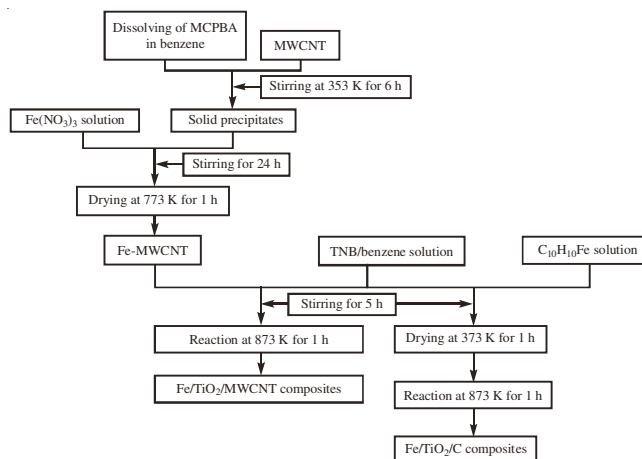


Fig. 1. Preparation procedure of Fe/TiO<sub>2</sub>/carbon composites

state and structure of Fe/TiO<sub>2</sub>/carbon composites using an electron microscope (JSM-5200 Jeol, Japan). TEM (Jeol, JEM-2010, Japan) at an acceleration voltage of 200 kV was used to investigate the size and distribution of the ferric and titanium deposits on the carbon surface of various samples. TEM specimens were prepared by placing a few drops of the sample solution on a carbon grid. EDX spectra were also obtained for determining the elemental information of Fe/TiO<sub>2</sub>/carbon composites. UV-Vis absorption parameters for the methylene blue solution degraded by Fe/TiO<sub>2</sub> and Fe/TiO<sub>2</sub>/carbon composites were recorded by a UV-vis (Optizen Pop Mecasys Co., Ltd., Korean) spectrophotometer. The UV light source was a 20 W lamp ( $\lambda = 365$  nm). The visible light source was an 8 W LED lamp ( $\lambda > 420$  nm, Fawoo Technology, Korea).

**Photocatalytic activity of samples:** The photocatalytic decomposition was tested by Fe/TiO<sub>2</sub> and different Fe/TiO<sub>2</sub>/carbon composites powder and an aqueous solution of methylene blue in a 100 mL glass container and then irradiating the system with UV with H<sub>2</sub>O<sub>2</sub> ( $1.5 \times 10^{-4}$  mol) and without H<sub>2</sub>O<sub>2</sub> and visible light, which was used at the distance of 100 mm from the solution in darkness, respectively. The sample powder of 0.03 g was suspended in the 50 mL of methylene blue solution with a concentration of  $1 \times 10^{-5}$  M. Then, the mixed solution was placed in the dark for at least 2 h, in order to establish an adsorption-desorption equilibrium, which was hereafter considered as the initial concentration (*c*<sub>0</sub>) after dark adsorption. Then, experiments were carried out under UV only and under UV with addition of  $1.5 \times 10^{-3}$  mol H<sub>2</sub>O<sub>2</sub> to the methylene blue solution (UV, visible light and UV + H<sub>2</sub>O<sub>2</sub>, respectively). Solution was then withdrawn regularly from the reactor by an order of 30, 60, 90 and 120 min, afterwards, 10 mL of solution was taken out and immediately centrifuged to separate any suspended solids. The clean transparent solution was immediately analyzed by using a UV-vis spectrophotometer in order to decrease continual oxidation of H<sub>2</sub>O<sub>2</sub> for methylene blue residue. The intensity at 660 nm for each sample was recorded.

## RESULTS AND DISCUSSION

**Structure and morphology:** The value of BET surface area of pure TiO<sub>2</sub>, Fe/TiO<sub>2</sub>, Fe/TiO<sub>2</sub>/C and Fe/TiO<sub>2</sub>/MWCNT composites are presented in Table-1 and were ordinal denoted as T, CT, FC1T and FC2T, respectively. As the results of Table-1,

TABLE-1  
BET SURFACE AREA AND EDX ELEMENTAL  
MICROANALYSIS (wt %) OF PURE TiO<sub>2</sub>, Fe/TiO<sub>2</sub> AND  
Fe/TiO<sub>2</sub>/C COMPOSITES

Samples	Nomen- clatures	S <sub>BET</sub> (m <sup>2</sup> /g)	Elements (wt %)			
			C	O	Ti	Fe
TiO <sub>2</sub>	T	8.3	–	19.57	80.43	–
Fe/TiO <sub>2</sub>	FT	11.9	–	55.45	43.44	1.11
Fe/TiO <sub>2</sub> /C	FC1T	25.6	8.53	33.71	56.32	1.44
Fe/TiO <sub>2</sub> /MWCNT	FC2T	33.3	10.37	24.97	62.92	1.74

the BET surface areas of pristine TiO<sub>2</sub> and Fe-TiO<sub>2</sub> were 8.3 and 11.9 m<sup>2</sup>/g, respectively. While the BET surface areas of Fe/TiO<sub>2</sub>/C and Fe/TiO<sub>2</sub>/MWCNT increased to 25.6 and 33.3 m<sup>2</sup>/g. When carbon compounds were introduced in Fe/TiO<sub>2</sub> composites, it can be evidently seen that there was large change of the micropore size for Fe/TiO<sub>2</sub>/C and Fe/TiO<sub>2</sub>/MWCNT composites compared to that of corresponding Fe/TiO<sub>2</sub>. This indicated that the supported carbon was directly related to adsorption ability of TiO<sub>2</sub>.

The SEM images of the Fe/TiO<sub>2</sub> and Fe/TiO<sub>2</sub>/carbon composites are shown in Fig. 2. Fig. 2(a-b) showed that the Fe/TiO<sub>2</sub> particles are nearly round in shape. It is clear that the nanoparticles were agglomerated to some extent and the rough measurements of images show that the average size of particles is in the nanoscale range. The SEM images of Fe/TiO<sub>2</sub>/C composite are shown in Fig. 2(c-d), the smooth surface of Fe/TiO<sub>2</sub>/C composite with a little bit granular aggregates of particles distributed in irregular shapes were observed, it revealed that the particles are compact, uniform, no cracks and no abnormality, which can be attributed to the growth and densification of carbon when treated at 873 K in air atmosphere. The morphological characterization of the Fe/TiO<sub>2</sub>/MWCNT composites was presented in Fig. 2 (e-f). These micrographs showed the general morphology of MWCNT and which was decorated with well-dispersed TiO<sub>2</sub> particles. Moreover, TiO<sub>2</sub> particles were also uniformly distributed on surface of MWCNT, which possibly are well homogenized during vigorous stir. It is considered that better dispersion enables larger number of active catalytic centers for the photocatalytic reaction<sup>19</sup>.

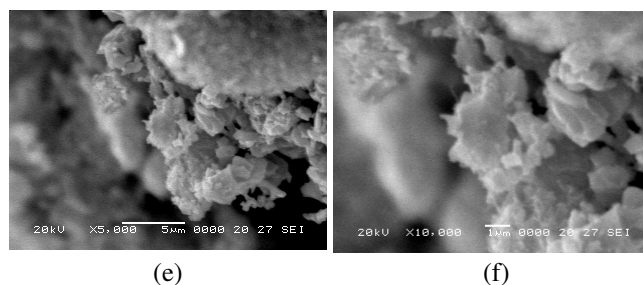
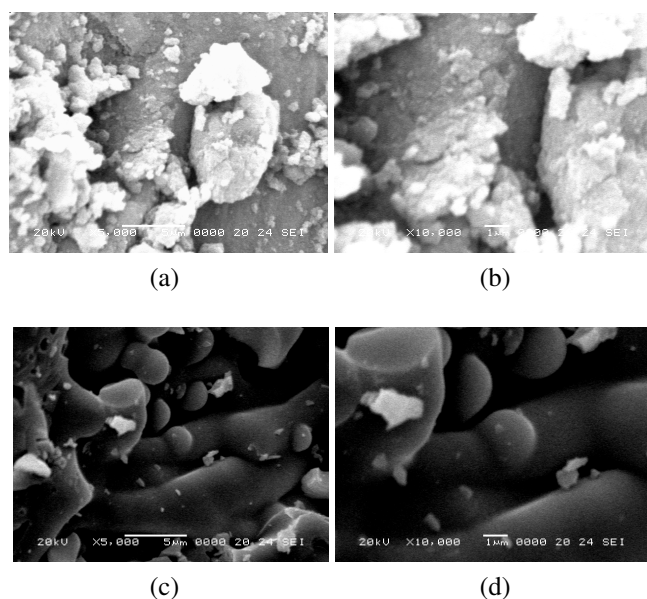


Fig. 2. SEM micrographs of Fe/TiO<sub>2</sub>, Fe/TiO<sub>2</sub>/carbon composites: Fe/TiO<sub>2</sub>: (a) × 5000, (b) × 10000, Fe/TiO<sub>2</sub>/C: (c) × 5000, (d) × 10000 and Fe/TiO<sub>2</sub>/MWCNT (e) × 5000, (f) × 10000

The TEM images of the Fe/TiO<sub>2</sub> and Fe/TiO<sub>2</sub>/carbon composites are measured in Fig. 3. A few black dots can be observed from these images in Fig. 3, correspond to the deposition of Fe particles. The TEM images of the Fe/TiO<sub>2</sub> composite showed that the size of TiO<sub>2</sub> particle observed was about 10-20 nm in Fig. 3(a). The TEM images of the Fe/TiO<sub>2</sub>/C composite [Fig. 3(b)] showed TiO<sub>2</sub> particles with the diameters of a few nm. These results suggest that the Fe/TiO<sub>2</sub>/C composites were composed of nano-sized TiO<sub>2</sub> and Fe particles in the matrix of carbon clusters. The Fe/TiO<sub>2</sub>/MWCNT composites were investigated by TEM to obtain additional information about the interfacial region of MWCNT crystals and surface areas. Fig. 3(c) showed that the surface areas of Fe/TiO<sub>2</sub>/MWCNT composites should be a strong interphase structural effect between the carbon and metal oxide phases. Occasionally a 0.1-0.5 nm thin layer was observed at the periphery of the MWCNT crystals.

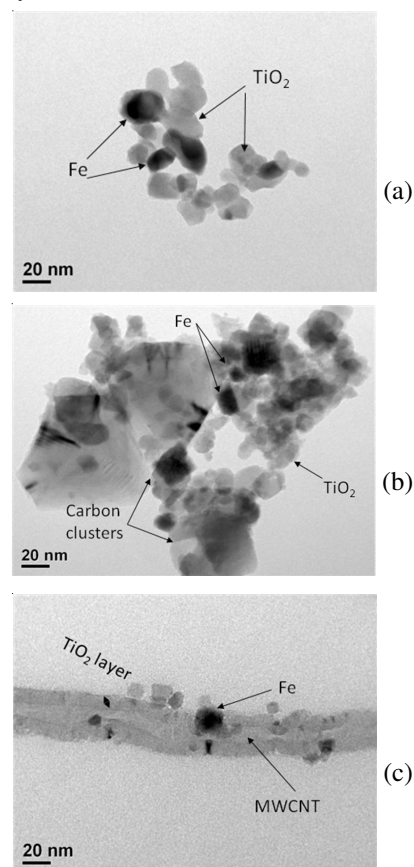


Fig. 3. TEM micrograph of the Fe/TiO<sub>2</sub> and Fe/TiO<sub>2</sub>/carbon composites: (a) Fe/TiO<sub>2</sub>, (b) Fe/TiO<sub>2</sub>/C, (c) Fe/TiO<sub>2</sub>/MWCNT

The XRD patterns are given in Fig. 4. In the case of the Fe/TiO<sub>2</sub>/carbon composites, the additional peaks presented in all the diffractograms correspond to the single anatase form of TiO<sub>2</sub>. The XRD results illuminated that the C and MWCNT in Fe/TiO<sub>2</sub>/carbon composites is similarly coated with a typical single anatase crystallites. The intense peaks of carbon correspond to the (002) reflection and to the (10) band. It could be noticed that the (101) anatase reflection overlaps the (002) reflection of carbon. In XRD patterns of the Fe/TiO<sub>2</sub>, significant diffraction peaks of rutile-phase TiO<sub>2</sub> were detected. It reflected that the carbon suppressed phase transformation from anatase to rutile during heat treatment at high temperature. According to the former study<sup>20</sup>, pure anatase nanocrystallites are very efficient photocatalysts, causes their superior photocatalytic properties. Especially, pure maghemite ( $\gamma$ -Fe<sub>2</sub>O<sub>3</sub>) and uniform peaks of 'FeO + 2TiO<sub>2</sub>' could be obtained at Fe/TiO<sub>2</sub> and Fe/TiO<sub>2</sub>/carbon composites, which indicated that the Fe/TiO<sub>2</sub> was successfully embedded in C and MWCNT matrix by present experimental method.

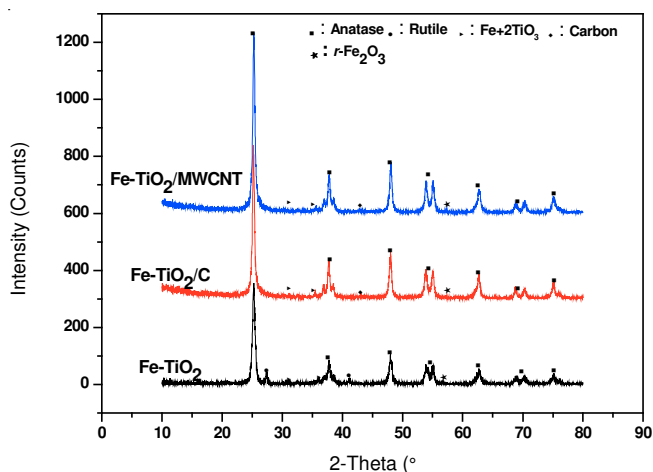
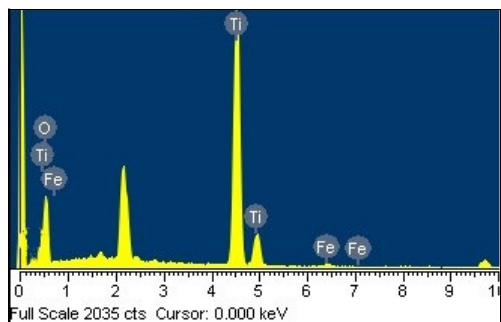
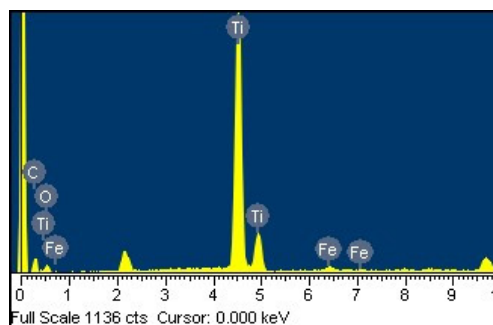


Fig. 4. XRD patterns of Fe/TiO<sub>2</sub> and Fe/TiO<sub>2</sub>/carbon composites

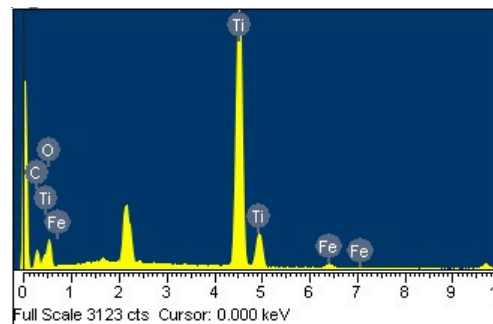
Fig. 5 shows the results of the EDX for Fe/TiO<sub>2</sub> and Fe/TiO<sub>2</sub>/carbon composites. These spectra showed the presence of peaks from the C, O, Ti and Fe elements. And, the numerical contents for the various elements are shown in Fig. 5 (Table-1). It showed that the quantities of carbon and Fe in the Fe/TiO<sub>2</sub>/carbon composites were small with a major element of Ti. According to former studies<sup>21,22</sup>, the higher concentration of dopant modified TiO<sub>2</sub> can be detrimental in formation of hole/electron recombination centers and an increase of negative charge capabilities.



(a)



(b)



(c)

Fig. 5. EDX elemental microanalysis of Fe/TiO<sub>2</sub> and Fe/TiO<sub>2</sub>/carbon samples: (a) Fe/TiO<sub>2</sub> (b) Fe/TiO<sub>2</sub>/C and (c) Fe/TiO<sub>2</sub>/MWCNT

### Degradation effects

**Adsorption ability:** Adsorption of organic dyes on the TiO<sub>2</sub> surface is an important parameter in heterogeneous photocatalysis. To evaluate the adsorption ability of pure TiO<sub>2</sub>, Fe/TiO<sub>2</sub> and Fe/TiO<sub>2</sub>/carbon samples, degradation of methylene blue solution was run under dark condition which is graphically illustrated in Fig. 6. From the Fig. 6, it is clear that degradation of methylene blue of Fe/TiO<sub>2</sub>/carbon is higher than that of pure TiO<sub>2</sub> and Fe/TiO<sub>2</sub> powders. This can be attributed to the large surface area of the Fe/TiO<sub>2</sub>/carbon composites due to introduction of C or MWCNT, which correlates to a strong adsorption ability. In addition, adsorption ability of the Fe/TiO<sub>2</sub>/MWCNT composite is slightly higher than that of the Fe/TiO<sub>2</sub>/C composite. According to Fig. 1, it may be considered that the Fe/TiO<sub>2</sub>/MWCNT composites have a rough surface structure through introduction of an external MWCNT.

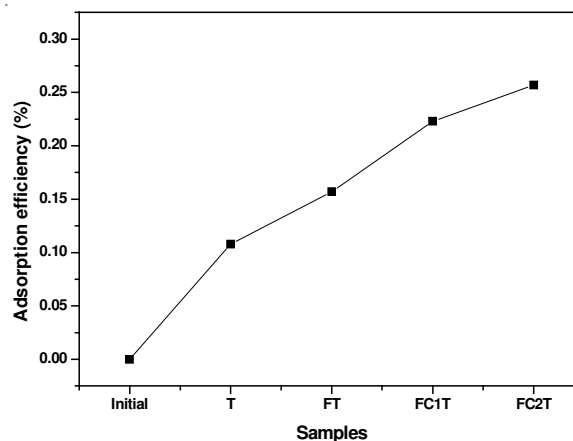


Fig. 6. Adsorption capability of pure TiO<sub>2</sub>, Fe/TiO<sub>2</sub> and Fe/TiO<sub>2</sub>/carbon samples for methylene blue under dark condition



**Photocatalytic activity under UV:** The relative methylene blue concentration  $c/c_0$  in natural logarithm scale is plotted in Fig. 7 against UV irradiation time on pure  $\text{TiO}_2$ ,  $\text{Fe/TiO}_2$ ,  $\text{Fe/TiO}_2/\text{C}$  and  $\text{Fe/TiO}_2/\text{MWCNT}$  sample. The relationship between  $-\ln(c/c_0)$  and time in Fig. 7 is approximately linear and so the rate constant  $k_{\text{app}}$  for degradation of methylene blue could be calculated for each sample from the line slope by following equation:

$$-\ln(c/c_0) = k_{\text{app}} t$$

where  $c_0$  and  $c$  are the initial concentration of methylene blue and the concentration at reaction time  $t$  (min), respectively.

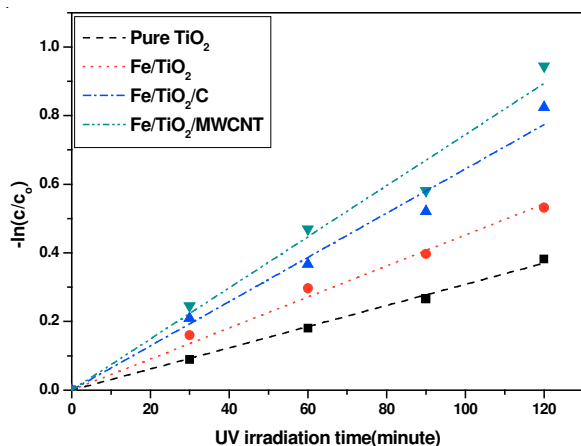


Fig. 7. Apparent first order kinetics of methylene blue degradation for pure  $\text{TiO}_2$ ,  $\text{Fe/TiO}_2$  and  $\text{Fe/TiO}_2/\text{carbon}$  composites under UV irradiation

The values of the rate constant ( $k_{\text{app}}$ ) are listed in Table-2. It was observed that photocatalytic performance of  $\text{Fe/TiO}_2$  composites for degradation of methylene blue is higher than that of pure  $\text{TiO}_2$ . Moreover, the  $\text{Fe/TiO}_2$  embedded in carbon matrix further improved photocatalytic activity.  $3.08$ ,  $4.52$ ,  $6.45$  and  $7.45 \times 10^{-3}$  of degradation rate was obtained with pure  $\text{TiO}_2$ ,  $\text{Fe/TiO}_2$ ,  $\text{Fe/TiO}_2/\text{C}$  and  $\text{Fe/TiO}_2/\text{MWCNT}$  samples in 2 h min under UV irradiation. The  $\text{Fe/TiO}_2$  composites showed a higher enhancement in the methylene blue photodegradation than that of pure  $\text{TiO}_2$ , which illuminated that the Fe particles is one of the vital factors in determining the photocatalytic performance of the catalysts under UV light irradiation. There are various reasons for the increase in the photocatalytic performance: (i) High photocatalytic activity of  $\text{Fe/TiO}_2$  composites may be related to high surface area. It is well known that the process is adsorption dependent, the photodegradation rate also increases. (ii) The effect of Fe particles on the photocatalytic activity under UV light irradiation should be due to the reason that the Fe particles can act as intermediates for

photo-generated holes and electrons transfer and inhibit the recombination of holes and electrons. (iii) The  $\text{Fe}^{3+}$  can work in photo-Fenton process in the following reactions:



When  $\text{Fe/TiO}_2$  was embedded in carbon matrix as C or MWCNT surface, the effect of carbon can enhance the surface area of  $\text{Fe/TiO}_2$  and transfer of electrons. The effect was clearly presented on both of  $\text{Fe/TiO}_2$  embedded in carbon matrix by a residue or an external carbon precursor. However, due to high electronic conductivity of MWCNT, the photodegradation rate of  $\text{Fe/TiO}_2/\text{MWCNT}$  composites is faster than that of  $\text{Fe/TiO}_2/\text{C}$  composites.

**Photocatalytic activity under the condition of UV +  $\text{H}_2\text{O}_2$ :** Degradation of methylene blue was also performed on the pure  $\text{TiO}_2$ ,  $\text{Fe/TiO}_2$  and  $\text{Fe/TiO}_2/\text{carbon}$  samples under UV irradiation in the presence of  $\text{H}_2\text{O}_2$ , which is used to initiate a photo-Fenton process. Degradation of methylene blue in the presence of  $\text{H}_2\text{O}_2$  without any photocatalyst under UV irradiation was carried out for comparison. The results with reaction time are first order as confirmed by the linear transforms as above equation shown in Fig. 8. The degradation rate of methylene blue on  $\text{Fe/TiO}_2/\text{carbon}$  was accelerated by addition of  $\text{H}_2\text{O}_2$ ;  $k_{\text{app}}$  for  $\text{Fe/TiO}_2/\text{C}$  and  $\text{Fe/TiO}_2/\text{MWCNT}$  composites is  $1.18$  and  $1.44 \times 10^{-2}$ , respectively. On the other hand, on pure  $\text{TiO}_2$  and  $\text{Fe/TiO}_2$ , degradation of methylene blue was slightly slower in the presence of  $\text{H}_2\text{O}_2$ , though it was still faster on  $\text{Fe/TiO}_2$  ( $k_{\text{app}} = 4.92 \times 10^{-3}$ ) than on pure  $\text{TiO}_2$  ( $k_{\text{app}} = 3.65 \times 10^{-3}$ ). Methylene blue was quickly degraded by  $\text{H}_2\text{O}_2$  without any photocatalyst employed ( $k_{\text{app}} = 5.43 \times 10^{-3}$ ), because  $\text{H}_2\text{O}_2$  is easily going upon photolysis yielding in OH radicals under UV irradiation as shown in reaction (2)<sup>23</sup>.

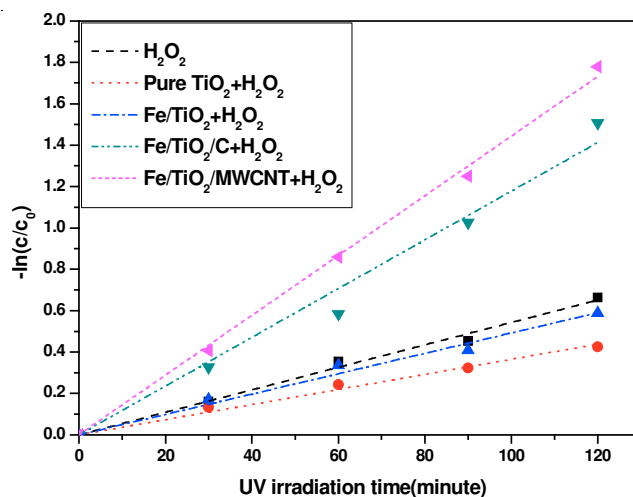


Fig. 8. Apparent first order kinetics of MB degradation for pure  $\text{TiO}_2$ ,  $\text{Fe/TiO}_2$  and  $\text{Fe/TiO}_2/\text{carbon}$  composites under UV irradiation with  $\text{H}_2\text{O}_2$

However, the  $\text{OH}^*$  radical formation on  $\text{TiO}_2$  and  $\text{Fe/TiO}_2$  in presence of  $\text{H}_2\text{O}_2$  could be decreased by the process of recombination of holes, which were formed on  $\text{TiO}_2$  or  $\text{Fe/TiO}_2$  surface after its excitation with electrons, which were supplied by  $\text{H}_2\text{O}_2$  [reaction (2)].

The behaviour of degradation of methylene blue on  $\text{Fe/TiO}_2/\text{carbon}$  composites was quite different from that on pure

Samples	$k_{\text{app}}$ ( $\text{min}^{-1}$ )		
	UV	UV + $\text{H}_2\text{O}_2$	Visible light
No sample	—	$5.43 \times 10^{-3}$	—
Pure $\text{TiO}_2$	$3.08 \times 10^{-3}$	$3.65 \times 10^{-3}$	$3.19 \times 10^{-4}$
$\text{Fe/TiO}_2$	$4.52 \times 10^{-3}$	$4.92 \times 10^{-3}$	$2.83 \times 10^{-3}$
$\text{Fe/TiO}_2/\text{C}$	$6.45 \times 10^{-3}$	$1.18 \times 10^{-2}$	$5.15 \times 10^{-3}$
$\text{Fe/TiO}_2/\text{MWCNT}$	$7.45 \times 10^{-3}$	$1.44 \times 10^{-2}$	$5.8 \times 10^{-3}$

TiO<sub>2</sub> and Fe/TiO<sub>2</sub>; for the formers the concentration of methylene blue solution drastically decreases with time of UV irradiation. A linear dependence is observed between the time of UV irradiation and the relative concentration of methylene blue solution,  $c/c_0$ . The speed of degradation of methylene blue in Fe/TiO<sub>2</sub>/carbon composites was supposed to be governed by the content of Fe<sup>2+</sup> and Fe<sup>3+</sup> in the photocatalysts and the redox processes of iron. In the presence of H<sub>2</sub>O<sub>2</sub>, Fe<sup>2+</sup> is very easily oxidized to Fe<sup>3+</sup>, according to reaction (3):



It was considered that under UV irradiation and in the presence of H<sub>2</sub>O<sub>2</sub> (condition of UV + H<sub>2</sub>O<sub>2</sub>) the formation of OH<sup>·</sup> radicals on Fe/TiO<sub>2</sub>/carbon composites increased due to the presence of Fe<sup>2+</sup> [reaction (3)], the higher amount of OH<sup>·</sup> radicals being formed on Fe/TiO<sub>2</sub>/carbon composites having the lower content of carbon<sup>12</sup>. Because of H<sub>2</sub>O<sub>2</sub> was adsorbed on the carbon surface<sup>11,24</sup>, therefore the amount of OH<sup>·</sup> radical formed due to the photolysis of H<sub>2</sub>O<sub>2</sub> was lower when the Fe/TiO<sub>2</sub>/carbon composites was used in presence of H<sub>2</sub>O<sub>2</sub> without the Fe/TiO<sub>2</sub>/carbon composites. Additionally OH<sup>·</sup> radical formation on the surface of TiO<sub>2</sub> was suppressed by the scavenging of the free carriers by H<sub>2</sub>O<sub>2</sub>.

**Photocatalytic activity under visible light:** Fig. 9 shows the photocatalytic degradation linear of methylene blue over the pure TiO<sub>2</sub>, Fe/TiO<sub>2</sub> and Fe/TiO<sub>2</sub>/carbon samples under visible light irradiation. The degradation rate of methylene blue on the pure TiO<sub>2</sub> is very low ( $k_{\text{app}} = 3.19 \times 10^{-4}$ ), which can be attributed to the self-sensitization of methylene blue molecules. Obviously, the photodegradation rate of Fe/TiO<sub>2</sub> ( $k_{\text{app}} = 2.83 \times 10^{-3}$ ) is superior to that of pure TiO<sub>2</sub>. Besides the self-sensitization of methylene blue molecules, the introductions of Fe species cause the absorption edge extended to visible light rang and thus play an important role in improving visible light photoactivity, although Fe/TiO<sub>2</sub> has slightly higher surface area than pure TiO<sub>2</sub>, as compared to the Fe/TiO<sub>2</sub> composite. The photodegradation effect of methylene blue with Fe/TiO<sub>2</sub> embedded in carbon matrix composites increased significantly (Fig. 9). Over the Fe/TiO<sub>2</sub>/MWCNT composite ( $k_{\text{app}} = 5.8 \times 10^{-3}$ ), the degradation rate of methylene blue is the highest.

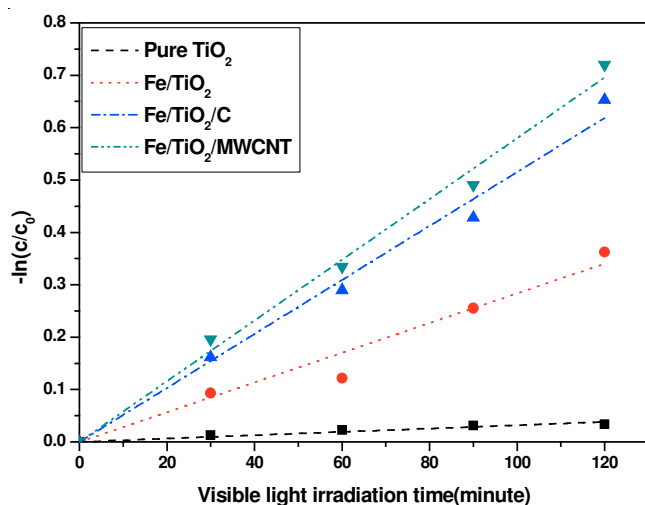
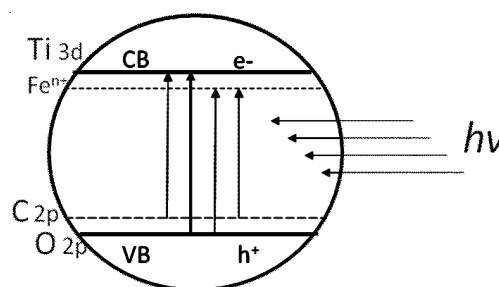


Fig. 9. Apparent first order kinetics of methylene blue degradation for pure TiO<sub>2</sub>, Fe/TiO<sub>2</sub> and Fe/TiO<sub>2</sub>/carbon composites under visible light irradiation

The higher photocatalytic activity of Fe/TiO<sub>2</sub> embedded in carbon matrix here observed may be attributed to the following reasons: (i) Carbon can act as electron recipient to effectively inhibit the recombination of electron/hole pairs. (ii) The specific surface area of Fe/TiO<sub>2</sub>/carbon composites was larger than that of Fe/TiO<sub>2</sub> which may favour the adsorption of methylene blue molecules as well as provide more possibly accessible active sites. (iii) The carbon introduced is supposed to create several localized midgap/surface states above the TiO<sub>2</sub> valence band rendering visible light absorption. (iv) The most important reason is that Fe and carbon have synergistic effects on improving visible light photoactivity.

Here we proposed a possible mechanism for the synergistic effects of Fe and carbon, which is illustrated in **Scheme-I**. **Scheme-I** showed that introduction of carbon could create intra-band-gap states close to the valence band edges. Simultaneously, Fe ion present in the substitution positions into the lattice of TiO<sub>2</sub> would introduce new energy level between the conduction and valence band of TiO<sub>2</sub>, which leads to a narrower band gap<sup>25</sup>. However, MWCNT is more reasonable to acts as photosensitizer, which is energetic enough and read to inject one electron through the coordinating bands to the conduction band of TiO<sub>2</sub> rather than poor C. Considering the semiconductive properties of MWCNT, which may absorb the irradiation and transfer the photo-induced electron (e<sup>-</sup>). Therefore, the photocatalytic activity of the Fe/TiO<sub>2</sub>/MWCNT composite is higher than that of the Fe/TiO<sub>2</sub>/C composite under visible light irradiation.



**Scheme-I:** Mechanism for the synergistic effects of Fe and carbon

## Conclusion

The Fe/TiO<sub>2</sub>/carbon composites with and without an external carbon precursor have been successfully prepared by a conventional sol-gel method. Methylene blue photocatalytic degradation on Fe/TiO<sub>2</sub>/carbon composites is faster than on TiO<sub>2</sub> and Fe/TiO<sub>2</sub> due to high surface area and facile transfer of electrons. Acceleration of degradation of methylene blue can be occurred on Fe/TiO<sub>2</sub>/carbon composites under UV upon addition of H<sub>2</sub>O<sub>2</sub> due to in presence of circulatory photo-Fenton system. The Fe/TiO<sub>2</sub>/carbon composites also presented higher photocatalytic activity under visible light irradiation.

## REFERENCES

1. C.G. Silva, W. Wang and J.L. Faria, *J. Photochem. Photobiol. A: Chem.*, **181**, 314 (2006).
2. V. Shah, P. Verma, P. Stopka, J. Gabriel, P. Baldrian and F. Nerud, *Appl. Catal. B: Environ.*, **46**, 287 (2003).
3. I.K. Konstantinou and T.A. Albanis, *Appl. Catal. B: Environ.*, **42**, 319 (2003).

4. T. Sauer, G.C. Neto, H.J. Jose and R.F.P.M. Moreira, *J. Photochem. Photobiol. A: Chem.*, **149**, 147 (2002).
5. B. Tryba, M. Piszcz, B. Grzmil, A. Pattek-Janczyk and A.W. Morawski, *J. Hazard. Mater.*, **162**, 111 (2009).
6. F. Lin, D.M. Jiang and X.M. Ma, *J. Alloys. Compounds*, **470**, 375 (2009).
7. J. Arana, O.G. Diaz, M.M. Saracho, J.M. DonaRodriguez, J.A. Herrera Melian and J.P. Pena, *Appl. Catal. B: Environ.*, **32**, 49 (2001).
8. C. Wang, D.W. Bahnemann and J.K. Dohrmann, *Chem. Commun.*, **16**, 1539 (2000).
9. J.A. Navio, G. Colon, M. Macias, C. Real and M.I. Litter, *Appl. Catal. A: Gen.*, **177**, 111 (1999).
10. X.H. Qi, Z.H. Wang, Y.Y. Zhuang, Y. Yu and J.L. Li, *J. Hazard. Mater.*, **118**, 219 (2005).
11. K. Zhang and W.C. Oh, *Kor. J. Mater. Res.*, **9**, 481 (2009).
12. B. Tryba, A.W. Morawski, M. Inagaki and M. Toyoda, *Chemosphere*, **64**, 1225 (2006).
13. S. Sakthivel and H. Kisch, *Angew. Chem. Int. Ed.*, **42**, 4908 (2003).
14. W.D. Wang, P. Serp, P. Kalck and J. Lu's Faria, *J. Mol. Catal. A: Chem.*, **235**, 194 (2005).
15. H. Matsui, S. Nagano, S. Karuppuchamy and M. Yoshihara, *Curr. Appl. Phys.*, **9**, 561 (2009).
16. H. Miyazaki, H. Matsui, T. Nagano, S. Karuppuchamy, S. Ito and M. Yoshihara, *Appl. Surface Sci.*, **254**, 7365 (2008).
17. F.J. Zhang, M.L. Chen, K. Zhang and W.C. Oh, *Bull. Kor. Chem. Soc.*, **31**, 133 (2010).
18. W.C. Oh, F.J. Zhang and M.L. Chen, *J. Ind. Eng. Chem.*, **16**, 321 (2010).
19. Y. Zhang, N. Kohler and M.Q. Zhang, *Biomaterials*, **23**, 1553 (2002).
20. M.L. Chen, J.S. Bae and W.C. Oh, *Anal. Sci. Tech.*, **19**, 460 (2006).
21. W.C. Hung, Y.C. Chen, H. Chu and T.K. Tseng, *Appl. Surface Sci.*, **255**, 2205 (2008).
22. L.C. Chen, Y.C. Ho, W.S. Guo, C.M. Huang and T.C. Pan, *Electrochim. Acta*, **54**, 3884 (2009).
23. B. Tryba, A.W. Morawski, M. Inagakic and M. Toyoda, *Appl. Catal. B: Environ.*, **63**, 215 (2006).
24. K. Zhang and W.C. Oh, *J. Kor. Ceramic Soc.*, **46**, 561 (2009).
25. Y.M. Wu, J.L. Zhang, L. Xiao and F. Chen, *Appl. Surface Sci.*, **256**, 4260 (2010).